Human crawling performance and technique revealed by inertial measurement units

Rachel V. Vitali *, Stephen M. Cain, Steven P. Davidson, Noel C. Perkins

Department of Mechanical Engineering, University of Michigan, Ann Arbor, MI, USA

ABSTRACT

Human crawling performance and technique are of broad interest to roboticists, biomechanists, and military personnel. This study explores the variables that define crawling performance in the context of an outdoor obstacle course used by military organizations worldwide to evaluate the effects of load and personal equipment on warfighter performance. Crawling kinematics, measured from four body-worn inertial measurement units (IMUs) attached to the upper arms and thighs, are recorded for thirty-three participants. The IMU data is distilled to four metrics of crawling performance; namely, crawl speed, crawl stride time, ipsilateral limb coordination, and contralateral limb coordination. We hypothesize that higher performance (as identified by higher crawl speeds) is associated with more coordinated limbs and lower stride times. A cluster analysis groups participants into high and low performers exhibiting statistically significant differences across the four performance metrics. In particular, high performers exhibit superior limb coordination associated with a "diagonal gait" in which contralateral limbs move largely in-phase to produce faster crawl speeds and shorter crawl stride times. In contrast, low performers crawl at slower speeds with longer crawl stride times and less limb coordination. Beyond these conclusions, a major contribution of this study is a method for deploying wearable IMUs to study crawling in contextually relevant (i.e. non-laboratory) environments.

© 2018 Elsevier Ltd. All rights reserved.

1. Introduction

Crawling represents a form of quadrupedal gait often employed by humans, reptiles, amphibians, and insects, among other organisms. A gait pattern is defined by Song and Waldron (1989) as "the time and the location of the placing and lifting of each foot, coordinated with the motion of the body in its six degrees of freedom, in order to move the body from one place to another." Relative to this definition, McGhee (1968) notes over 5000 possible quadruped gaits, including trotting, galloping, and crawling that are considerably more common than others. One common form of crawling gait consists of a diagonal interlimb pattern where the limbs (e.g., arms and legs) on opposite sides of the body swing in unison (Adolph et al., 1998; Patrick et al., 2009). Diagonal gait has further implications in designing controllers for quadruped robots, which may leverage gait transitions observed in nature to improve performance (Kano et al., 2012; Owaki et al., 2012; Owaki and Ishiguro, 2017). For example, several species of lizards exhibit

diagonal gait when transitioning to high speeds, and it is further believed that diagonal gait affords greater stability and maneuverability (McElroy et al., 2008).

Diagonal crawling gait is commonly observed in humans and marks important motor learning gains during infant development (Adolph et al., 1998; Patrick et al., 2009; Patrick et al., 2012). Infants generally transition from crawling with their abdomen contacting the floor to crawling with contact solely through their hands and knees, which introduces new neural, biomechanical, and task constraints contributing to the challenges of maintaining balance and support (Freedland and Berthenthal, 1994). Despite these challenges, infants observed in a longitudinal study systematically converge to the same diagonal interlimb gait (Freedland and Bertenthal, 1994). Crawling balance and dynamic stability follow from a base of support formed with as few as two limbs contacting the ground (Raibert 1986). Diagonal crawling gait yields a diagonal base of support that remains nominally beneath the mass center. Studies of infant crawling suggest that the diagonal gait pattern may also yield the most dynamically stable crawling gait as it minimizes side to side variation of the mass center relative to the (diagonal) base of support (Adolph et al., 1998).

* Corresponding author at: Department of Mechanical Engineering, University of Michigan, Ann Arbor, 2350 Hayward St, Ann Arbor, MI 48109, USA.
E-mail address: vitalir@umich.edu (R.V. Vitali).

Additional studies explore the effect of limb length on diagonal gait. For example, short-legged animals (e.g., amphibians, reptiles, and short-legged mammals) adopt diagonal gait for greater stability per the aforementioned reason (Hildebrand 1989). The same holds for infants who preferentially adopt a wide stance with respect to their shoulder width by placing their limbs further from the sagittal plane (Patrick et al., 2009). Relative to adults, infants have proportionally shorter limbs and adapt to relatively poorer balance by widening their base of support. When adults are forced to widen their base of support (limbs forced further from sagittal plane via obstructions), they converge to using the same diagonal crawling gait of infants (Patrick et al., 2009).

The objective of this study is to explore the variables that define and discriminate human crawling performance. We do so in the context of an outdoor obstacle course that embeds a crawling task for military personnel (Tack et al., 2012). Crawling of military personnel may signal functional capacity following injury (Cancio et al., 2017), expose the mechanisms and types of injury (Schermann et al., 2017; Schwartz et al., 2018), and optimize the size and configuration of carried loads (Jaworski et al., 2015; Larsen et al., 2012; Larsen et al., 2014; Mitchell et al., 2016; O'Neal et al., 2014). Historically, crawling performance for military assessment is quantified solely by the time required to complete a crawling task. Although completion time is an important measure of performance, it does not reveal the techniques used or the underlying biomechanical motions that contribute to superior performance. For example, (Larsen et al., 2012; Larsen et al., 2014) conclude that large added loads from body armor significantly increases completion time. However, completion time does not reveal any of the companion changes in the biomechanical movements as also noted by observation (Larsen et al., 2014). In this study, we explore crawling performance across four measures of crawling performance; namely, crawl speed, crawl stride time, ipsilateral limb coordination, and contralateral limb coordination. Building from the previous literature, we hypothesize that superior crawling performance, as defined by faster crawl speed, is associated with greater limb coordination and shorter crawl stride time. Importantly, we do so in the context of an outdoor (non-laboratory) environment by exploiting advances in body-worn inertial measurement units for motion capture.

2. Methods

2.1. Participants, equipment, and protocol

Thirty-three participants (19M/14F, 20.2 ± 2.0 yrs, 1.75 ± 0.12 m, 71.6 ± 14.2 kg) were recruited from a collegiate Reserve Officers' Training Corps (ROTC) and club sports population. The University of Michigan Institutional Review Board approved the study and participants gave informed consent. Participants wore an array of inertial measurement units (IMUs) (Opal, APDM, Portland, OR, USA). Four IMUs attached to upper arms and thighs with arbitrary orientation are pertinent to this study (Fig. 1). Each IMU includes a triaxial accelerometer (6 g range, 14-bit resolution, 650 μg/√Hz noise floor) and a triaxial angular rate gyro (2000°/s range, 16-bit resolution, 0.03°/s/√Hz noise floor) sampled at 128 Hz. We employ inertial motion capture to avoid the limitations of traditional optical motion capture such as limited capture volume, marker occlusion, and restriction to a laboratory setting.

Participants completed a crawling task as part of a larger outdoor obstacle course modeled after the Load Effects Assessment Program (LEAP); see, for example, (Tack et al., 2012; Mitchell et al., 2016). The LEAP obstacle course is used by military organizations worldwide to evaluate the effects of load and other personal equipment on warfighter performance. It was created to replicate
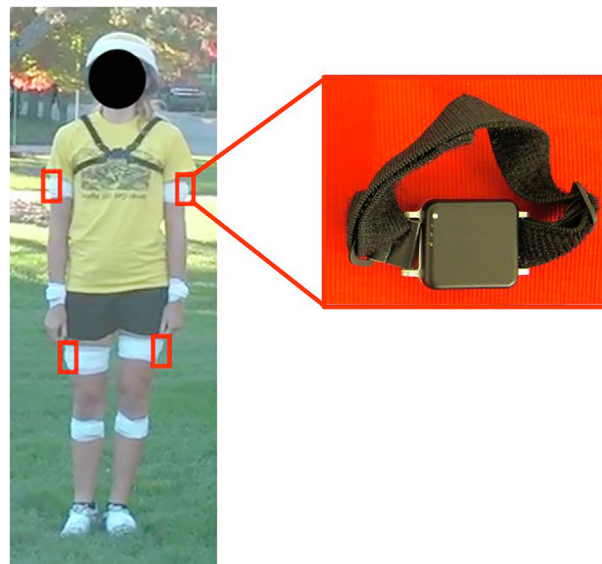

Fig. 1. Participant with four IMUs attached to upper arms and thighs (red boxes) and a callout of an IMU node on the right.

the common movements of warfighters and was specifically designed by the U.S. military to incorporate motions and tasks important for military personnel as emphasized in Tack et al. (2012) and Mitchell et al. (2016). The additional IMUs visible in Fig. 1 were employed to resolve the motion of additional body segments pertinent to other obstacles in the course as reported, for example, in Cain et al. (2016) for the balance beam obstacle, in McGinnis et al. (2017) and Zaferiou et al. (2017) for the agility run obstacle, in McGinnis et al. (2016) for the vertical jump obstacle, in Tammana et al. (2018) for the vertical load transfer obstacle (a lifting task), and in Ojeda et al. (2017) for the stair case run obstacle.

In the context of the LEAP, the crawling task in this study is referred to as the high crawl. Participants started each crawl trial prone with their elbows even with a set of cones and were instructed to crawl to another set of cones 9.1 m (30 ft) away while keeping their body as low to the ground as possible. In so doing, participants crawled on their elbows (not hands) and knees, though they also used their feet as additional points of contact when moving forward; refer to sample videos in the Supplementary Material. Participants also cradled a mock rifle weighing 7 lbs (3.18 kg) between their forearms and biceps while crawling. Prior to the data collection, participants practiced their crawling technique to reduce learning effects.

2.2. Analysis of IMU data

Analysis of the IMU data begins by parsing the data into crawling gait cycles by detecting events that define the start and end of each cycle. Subsequent analysis of the parsed cycles reveals the speed of crawling and coordination of the upper and lower limbs. These metrics, described next, are analogous to prior measures for crawling (see, for example, McElroy et al., 2008; Patrick et al., 2009; Patrick et al., 2012; Righetti et al., 2015). Crawling performance is then examined using a cluster analysis that discriminates the crawling speed and coordination of high performing participants where performance is first defined by the traditional measure of time to complete the crawling task. Further statistical analyses confirm significant differences in speed and coordination

metrics between the high and low performance groups. A description of each of these four steps follows.

Step 1: Crawl gait event definition and detection

The IMU data is parsed into individual gait cycles via the acceleration sampled at both upper arms. In particular, the acceleration magnitude at an upper arm exhibits a pronounced peak each time the associated elbow strikes the ground. These peaks readily define the start and end of each crawling gait cycle (Fig. 2).

By contrast, the acceleration sampled on each thigh does not readily distinguish gait cycles as the acceleration for the associated knee strikes can be significantly attenuated relative to the elbow strikes. Additionally, the knee often slips on the ground further confounding the detection of the cycle (refer to the high performer video in the Supplementary Material). Nevertheless, the motion of the thigh, and particularly the phasing of the motion of each thigh relative to both upper arms is critical to crawling performance. This phasing is captured by the coordination metrics proposed below.

Step 2: Crawl speed and stride time

The crawl is bookmarked by the first and last elbow strikes, which define the crawl completion time (Fig. 2). The length of the crawl (9.1 m) divided by the crawl completion time yields the average crawl speed. Stride times are defined from sequential elbow impacts on the same arm (i.e. time from one left elbow impact to the next left elbow impact); refer to Fig. 2. For each participant, the stride time is reported as the mean of the stride times for both right and left upper arms.

Step 3: Ipsilateral and contralateral coordination metrics

Two different (but related) metrics of crawl coordination are defined in this study; namely ipsilateral and contralateral coordination. Ipsilateral coordination measures the phasing of limbs on the same side of the body (e.g., phasing of the right thigh relative to the right upper arm). Contralateral coordination measures the phasing of limbs on the opposite side of the body (e.g., phasing of the left thigh relative to the right upper arm). These coordination metrics are computed from the angular velocities measured synchronously on all four limbs as follows.

First, the principal axis of rotation for each upper arm during each stride is estimated from a principal component analysis (PCA) (Wold et al., 1987) of each upper arm's angular velocity data.

The PCA returns three orthogonal axes that describe the variation in angular velocity where the first axis captures the majority of the variation and is used as the principal axis of rotation. Additionally, the resulting principal axis nominally points in the lateral direction. The angular velocity for each upper arm is projected onto the associated principal axis of rotation to yield "arm principal angular velocities" $\omega_{arm,i}$ where $i = l$ or r for *left* or *right* upper arm. An analogous procedure is followed for the angular velocity measured from each thigh-mounted IMU, with one important difference. This PCA for each thigh is conducted twice, once using the strides defined by the left elbow strikes and then again using the strides defined by the right elbow strikes. Doing so yields "leg principal angular velocities" $\omega_{leg,ij}$ where $i = l$ or r for *left* or *right* elbow strikes and $j = l$ or r for *left* or *right* thigh. For example, $\omega_{leg,rr}$ is the right thigh principal angular velocities using the strides defined by the right elbow strikes and $\omega_{leg,lr}$ is the right thigh principal angular velocities using the strides defined by the left elbow strikes. In summary, each of these scalar quantities describes the angular speeds of each limb about the principal axis of rotation of each limb.

Next, a coordination matrix β (2×2) is formed that measures the phasing of each pair of arm and leg principal angular velocities. The components of the coordination matrix are

$$\beta_{ij} = \frac{\int_{t_1}^{t_2} \omega_{arm,i}(t)\omega_{leg,ij}(t)dt}{\sqrt{\int_{t_1}^{t_2} \omega_{arm,i}(t)^2 dt}\sqrt{\int_{t_1}^{t_2} \omega_{leg,ij}(t)^2 dt}} \qquad (1)$$

where the limits of integration begin with the time of the first elbow strike (t_1) to the last elbow strike (t_2),i.e., the crawl completion time illustrated in Fig. 2. The component β_{ij} is a measure of the phase between the principal angular velocities of the *i*th upper arm and the *j*th thigh (calculated with the *i*th elbow strikes), where again $i, j = l(eft)$ or $r(ight)$. Note that $-1 \leq \beta_{ij} \leq 1$ and that the limiting values $\beta_{ij} = 1$ and $\beta_{ij} = -1$ denote perfectly in-phase and perfectly out-of-phase motions, respectively; refer to illustrative example in Fig. 3 for principal angular velocities that are sinusoids.
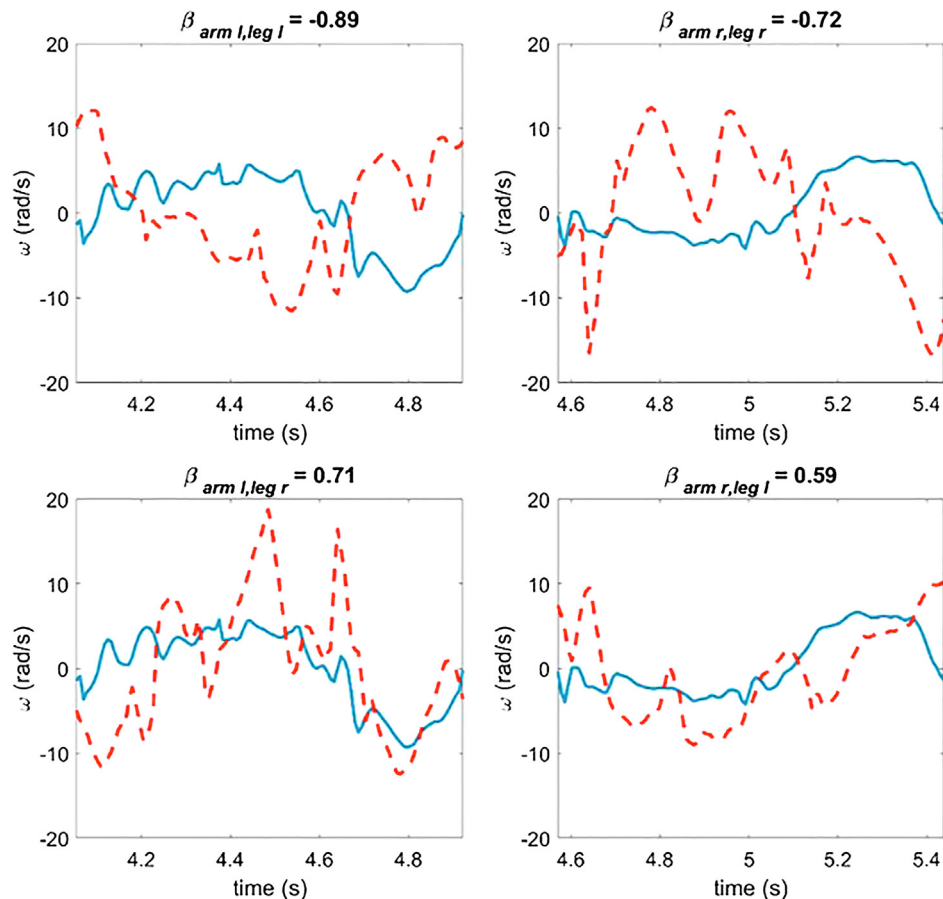
However, the principal angular velocities during crawling are not simple sinusoids as illustrated in the example of Fig. 4. Shown are principal angular velocities for each of the four limb combina-
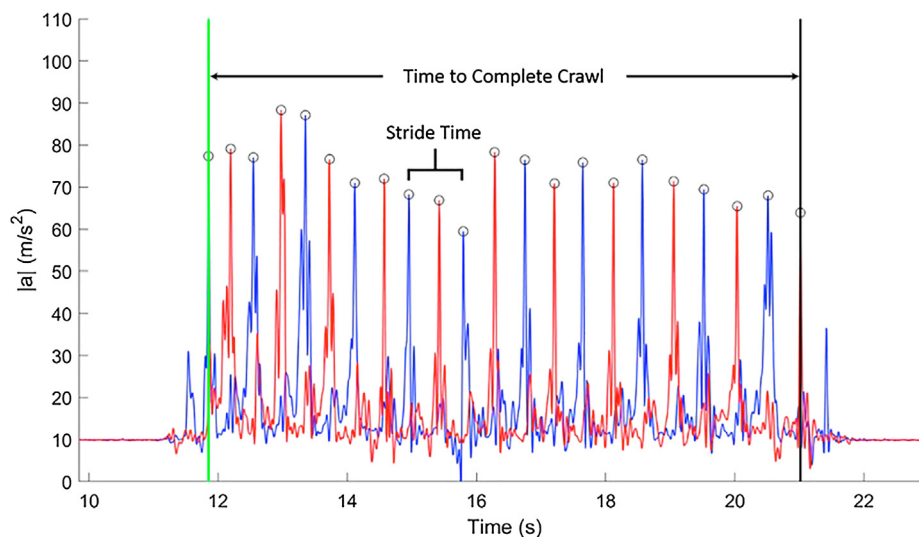
Fig. 2. A plot of the acceleration magnitudes (including superimposed gravity) of IMUs attached to left (blue) and right (red) upper arm. Circles denote elbow strikes for each arm. The vertical green line indicates the start of the crawl and the vertical black line indicates the end of the crawl. A single "stride" time is illustrated for the left arm.
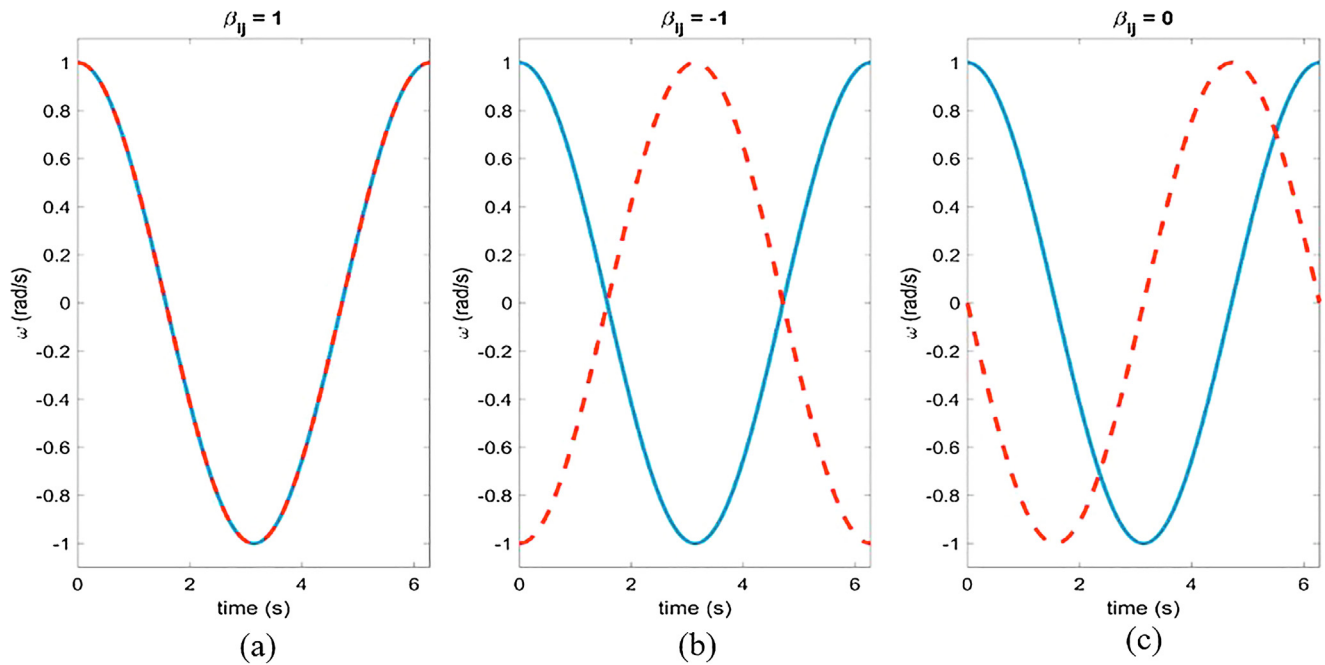
Fig. 3. Example illustrating the interpretation of the components of the coordination matrix for principal angular velocities described by two (phase-shifted) sinusoids having period 2π. In this case, β_{ij} reduces to $\cos\phi$ where ϕ is simply the phase angle between the two sinusoids. (a) $\beta_{ij} = 1$ for two principal angular velocities that are exactly in-phase ($\phi = 0$). (b) $\beta_{ij} = -1$ for two principal angular velocities that are exactly out-of-phase ($\phi = \pi$). (c) $\beta_{ij} = 0$ for two principal angular velocities that are out-of-phase by $\phi = \pi/2$.

Fig. 4. Representative principal angular velocities of the upper arms (blue) and thighs (dashed red) over a single stride for an exemplar high performer. If, for example, the right (left) upper arm is rotating counterclockwise (clockwise), the principal angular velocity is positive. The top row illustrates the relative phasing of the ipsilateral limbs and the bottom row illustrates the phasing of the contralateral limbs. The resulting components of the coordination matrix β_{ij} for this example stride are reported.

tions over a typical stride for an exemplar high performer. The associated components β_{ij} of the coordination matrix are also reported, and they include values suggesting significant out-of-phase limb motions (-0.89 and -0.72) as well as values suggesting significant in-phase limb motions (0.71, 0.59); refer to Discussion.

Next, we report the four components (β_{ij}) averaged across all strides and summarize those results in a "coordination map" as illustrated by the example shown in Fig. 5. The average values of β_{ij}(white circles) for each indicated pair of limbs are shown relative to the possible range of values $-1 \leq \beta_{ij} \leq 1$. In the coordination map, positive (negative) values of β_{ij} that lie in the upper (lower) half of the range signify limb phasing that tends towards in-phase (out-of-phase).

The coordination map of Fig. 5 is typical of a high performer as it reveals significant out-of-phase motion of the ipsilateral limbs ($\beta_{armr,legr} = -0.79$, $\beta_{arml,legl} = -0.83$) simultaneously with significant in-phase motion of the contralateral limbs ($\beta_{armr,legl} = 0.66$, $\beta_{arml,legr} = 0.76$). Leveraging this observation, we define two overall crawl coordination metrics that measure ipsilateral limb coordination

$$\beta_i = \frac{\beta_{armr,legr} + \beta_{arml,legl}}{2} \qquad (3)$$

and contralateral limb coordination

$$\beta_c = \frac{\beta_{armr,legl} + \beta_{arml,legr}}{2} \qquad (4)$$

Recall that the coordinate maps illustrated in Fig. 6 illustrate the ipsilateral and contralateral coordination averaged across all crawling cycles performed by the two exemplars.

Step 4: Cluster and statistical analysis

We explore how crawl speed, stride time, contralateral coordination, and ipsilateral coordination contribute to overall crawling performance and technique using a *k*-means cluster analysis. The optimal number of means is evaluated with a standard criteria known as the silhouette criterion (Rousseeuw, 1987), which provides a measure of how similar variables are within a cluster and how dissimilar they are across clusters. Prior to the cluster analysis, each of the four variables were normalized by their respective ranges to assign equal weighting in determining the clusters. After confirming normality, differences in the four variables between groups are further assessed with Welch's *t*-tests (to account for

unequal variances between groups) with statistical significance evaluated at $\alpha = 0.05$. These statistical tests are conducted to confirm the distinction of the groups identified by the cluster analysis.

3. Results

The silhouette coefficient (0.63) indicated a reasonable structure (Kaufman and Rousseeuw, 1990) that distributed the participants into two groups ($n_1 = 26$, $n_2 = 7$). Silhouette coefficients for the other numbers of clusters are reported in Table 1 of the Supplementary Material. The ratio of inter-cluster distance to intra-cluster distance (calculated using Euclidean L_2 norm distances (Kumar et al., 2014)) for crawl speed, crawl stride time, ipsilateral coordination, and contralateral coordination are 1.18, 1.19, 1.23, and 1.25, respectively. A ratio greater than 1 indicates that the parameter highly contributes to the group composition. Thus, in this case, each of the four variables contributes approximately equally. Table 1 below provides the descriptive statistics distinguishing the two clusters (or groups) from one another. The first cluster (Group 1) exhibits faster crawl speeds (denoting superior crawling performance), shorter crawl stride times, and coordination metrics closer to ±1 (denoting more coordinated limbs) as compared to the second cluster (Group 2). Shapiro-Wilk normality tests and q-q plots for all variables in both groups did not indicate any significant deviations from the normal distribution. Table 1 also provides the results of the Welch's *t*-tests. Importantly, Table 1 provides the effect sizes (Cohen's *d*) for the differences across the groups as referred to in the following discussion.

Differences in crawl speed, crawl stride time, and coordination across the groups reveal clear differences in performance. Moreover, the performance difference appears to manifest in differing crawling technique as identified by the coordination metrics discussed next.

4. Discussion

We hypothesized that superior crawling performance (as defined by faster crawl speed) is associated with greater limb coordination and shorter stride time. Confirming this hypothesis, the cluster analysis revealed one cluster (Group 1) was characterized by faster crawl speeds, shorter crawl stride times, and greater limb coordination. Additional statistical tests were conducted to further
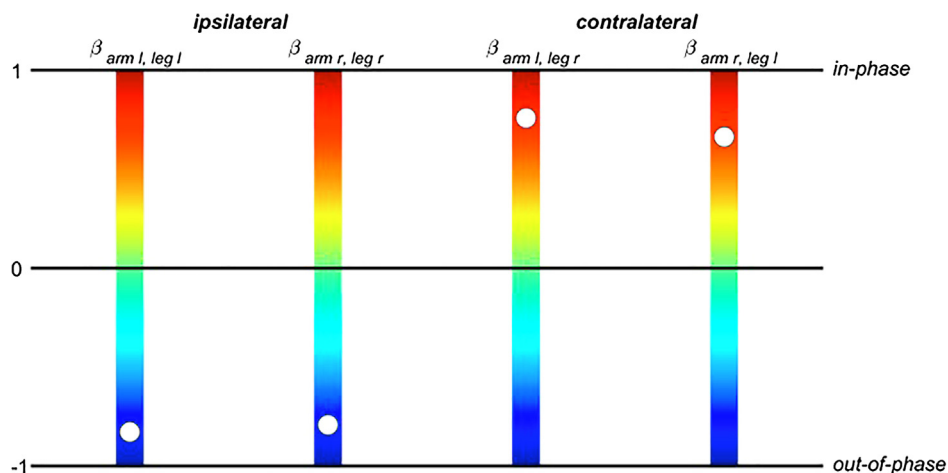
Fig. 5. Coordination map for exemplar high performer from Fig. 4 (refer also to high performer video in Supplementary Material). Components β_{ij} (averaged across all strides) of the coordination matrix (white dots) are shown relative to possible range -1(blue) $\leq \beta_{ij} \leq 1$(red). The upper half designates $\beta_{ij} > 0$ for phasing that tends towards in-phase; the lower half designates $\beta_{ij} < 0$ for phasing that tends towards out-of-phase.
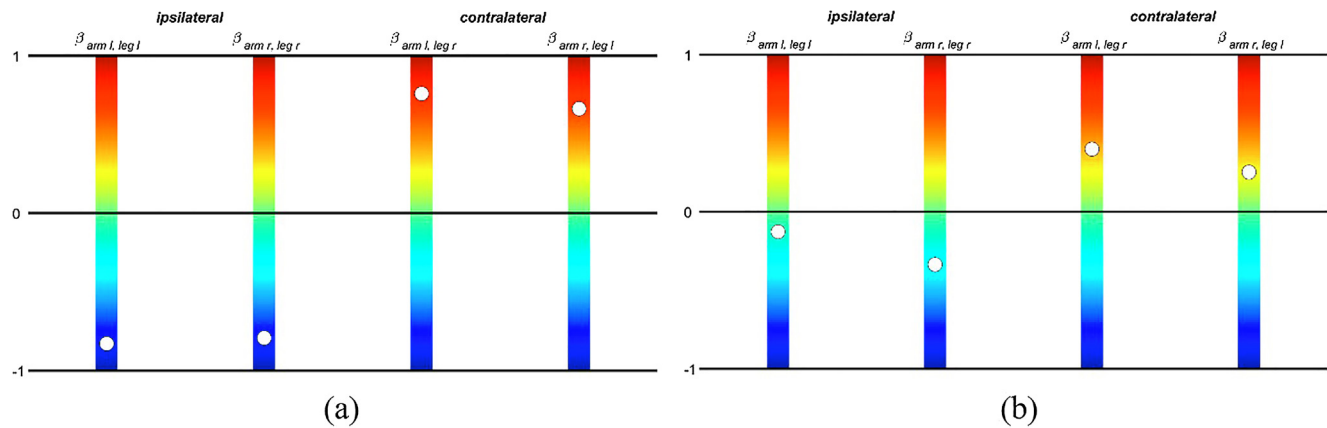
Fig. 6. Example coordination maps for an exemplar (a) high performer (refer to Fig. 5) and (b) low performer.

Table 1

Mean ± standard deviation of four crawl performance metrics for two groups identified by the cluster analysis. Performance metrics include average crawl speed, crawl stride time, ipsilateral coordination and contralateral coordination. The differences (Δ) denote Group 1 – Group 2. The t-statistic, p-value, and Cohen's d effect size results from the Welch's t-test.

|	Group 1	Group 2	Δ	t	p	d
Crawl Speed (m/s)	0.7 ± 0.2	0.5 ± 0.2	0.2	2.80	0.02[*]	1.09
Crawl Stride Time (s)	1.3 ± 0.2	1.8 ± 0.6	−0.6	−2.59	0.04[*]	−1.30
Ipsilateral Coordination	−0.63 ± 0.11	−0.27 ± 0.20	−0.37	−4.72	<0.01[†]	−2.29
Contralateral Coordination	0.57 ± 0.20	0.22 ± 0.37	0.35	2.42	0.04[*]	1.18

Significant at $\alpha = 0.05$[*], 0.01[†].

confirm the hypothesis and the distinction of the groups identified by the cluster analysis. The effect size for the crawl speeds (also average crawl completion time) suggests the two groups significantly differ by approximately one standard deviation ($d = 1.09$). The other speed related metric, crawl stride time, also significantly differs between the two groups with the stride times of the high performers (1.3 s) being significantly shorter than those of the low performers (1.8 s). Prior literature suggests the main strategy to increase speed is to decrease the stance duration (Patrick et al., 2012; Righetti et al., 2015), implying the duration of the swing phases largely remains the same across different speeds. If so, one can infer that high performers spend approximately half a second less (on average) in the stance phase compared to low performers. Note that the product of the average crawl speed and the average crawl stride time yields an estimate for the average crawl stride distance, which is 0.9 m for both high and low performers. This lends further support to the belief that the mechanics of the swing phase alone would not distinguish high from low performers (Patrick et al., 2012; Righetti et al., 2015).

The most prominent difference in performance is revealed by ipsilateral coordination. The substantial effect size ($d = -2.29$) suggests the mean ipsilateral coordination for the two groups differs by more than two standard deviations. Contralateral coordination also significantly differs between the two groups, but the associated effect size is about half that for ipsilateral coordination. Fig. 6 compares the coordination maps for an exemplar high performer (same as that of Fig. 5) adjacent to that of an exemplar low performer. For the exemplar high performer, the ipsilateral limbs are substantially out-of-phase (note the proximity of $\beta_{armr,legr}$ and $\beta_{arml,legl}$ to the blue end of the range where $\beta = -1$) while the contralateral limbs are substantially in-phase (note the proximity of $\beta_{armr,legl}$ and $\beta_{arml,legr}$ to the red end of the range where $\beta = 1$). In contrast, for the exemplar low performer, the limbs are neither substantially in-phase or out-of-phase (note the closer proximity of β_{ij} to the center of the map where $\beta = 0$).

It is also interesting to examine possible cycle-to-cycle variations of these coordination metrics. To that end, Fig. 7 reports the moving averages (average of right and left first stride, right and left second stride, etc.) of the ipsilateral and contralateral coordination for (a) the exemplar high performer and (b) the exemplar low performer. The moving average for the high performer exhibits rather small variation. Thus, the high performer crawls with highly consistent coordination and also with coordination components reasonably close to ± 1 as illustrated by the overall average as well as in Fig. 6(a). Conversely, considerable variation is observed in the moving average of the coordination components for the low performer, which suggests that the low performer does not crawl with consistent coordination stride to stride. Moreover, the averages of the coordination components are close to 0, as illustrated by the overall average and in Fig. 6(b).

Overall, the exemplar low performer's limbs do not exhibit strong limb pairing and the limbs largely move independently of each another in cyclic sequence. (Refer also to the exemplar low performer video in the Supplementary Material.) Consequently, members in the low performing group incur significantly longer stride times as, for example, they wait to move their thigh only after the preceding elbow strike. In other words, low performers incur added stance time while they wait for their legs to catch up with their arms. In contrast, the exemplar high performer's limbs remain strongly paired and with coordination that mimics the diagonal interlimb pattern often observed at faster locomotion speeds (McElroy et al., 2008; Patrick et al., 2009). (Refer also to the exemplar high performer video in the Supplementary Material.) Consequently, members in the high performing group crawl rapidly through superior ipsilateral and contralateral limb coordination. Indeed, the ipsilateral coordination is so strong that the ipsilateral limbs mimic the pairs of coupled oscillators previously observed in other modes of human locomotion (e.g., walking, creeping (i.e. crawling on hands and feet), and swimming) (Wannier et al., 2001). In all, the results from the additional statis-
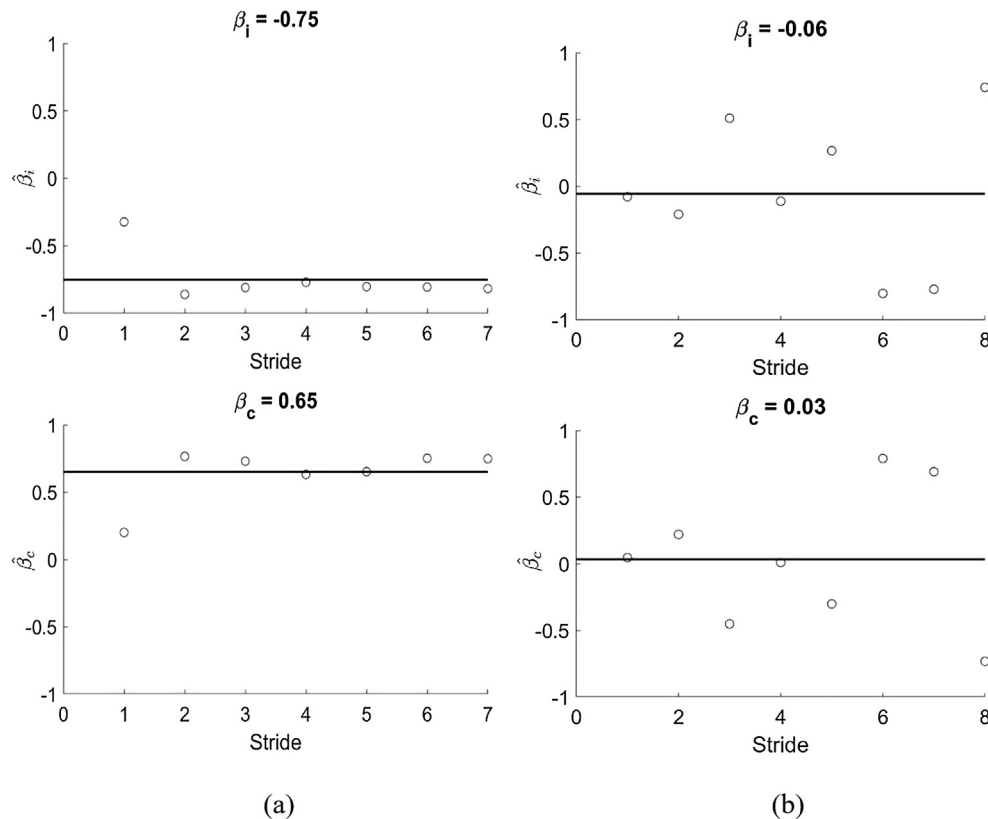
Fig. 7. Moving averages of ipsilateral ($\widehat{\beta}_i$) and contralateral coordination ($\widehat{\beta}_c$) for the exemplar (a) high performer and (b) low performer. The black lines represent the averages across the trial as reported in each figure's title.

tical tests further confirm the hypothesis that higher performance is associated with more coordinated limbs and lower stride times.

One factor that may contribute to participants' ability to coordinate their limbs could be the additional constraint of cradling the mock rifle in their arms. Cradling the mock rifle is an integral part of the testing protocol for the LEAP obstacle course (see, for example, (Mitchell et al., 2016)). In the exemplar high performer video (Supplementary Material), the mock rifle remains firmly secured between the forearms and biceps, essentially creating a rigid constraint between the forearms. Perhaps as a result, the arm movements remain nearly perfectly out-of-phase. In the exemplar low performer video (as well as videos of other members of the low performance group) the mock rifle is secured using one hand and the crook of the contralateral arm's elbow, rendering it considerably less stable (i.e., not a rigid constraint). The added distraction and attention to stabilizing the mock rifle may contribute to the observed poorer limb coordination.

5. Conclusions

This study contributes a novel method to measure and quantify crawling motion using four body-worn inertial measurement units attached to the upper arms and thighs. Doing so enables the study of crawling in relevant (non-laboratory) contexts including in an outdoor obstacle course frequently used by military organizations worldwide to evaluate the effect of load and other personal equipment on warfighter performance. The data harvested from the embedded inertial sensors (accelerometers and angular rate gyros) is used to construct four measures of crawling performance; namely, crawl speed, crawl stride time, ipsilateral limb coordination, and contralateral limb coordination. Ipsilateral and contralateral limb coordination quantify the phasing of the rotations of the upper arms and thighs, and thus they are also a product of the underlying motor control (not directly measured). Collectively, they reveal the purposeful, coordinated movements that contribute to superior (or inferior) crawling performance as further revealed in a cluster analysis that aggregates participants into (statistically significantly different) high and low performance groups. The results of the cluster analysis and statistical tests confirm the hypothesis that higher performance is associated with limb coordination and stride times. Overall, high performers exhibit superior limb coordination associated with a "diagonal gait" that produces faster crawl speeds and shorter crawl stride times. In contrast, low performers crawl at slower speeds with longer crawl stride times and with significantly less limb coordination.

Conflict of interest statement

The authors declare no conflict of interest.

Acknowledgements

Appendix A. Supplementary material

Supplementary data to this article can be found online at https://doi.org/10.1016/j.jbiomech.2018.12.030.

References

Adolph, K.E., Vereijken, B., Denny, M.A., 1998. Learning to crawl. Child Dev. 69 (5), 1299–1312.

Cain, S.M., McGinnis, R.S., Davidson, S.P., Vitali, R.V., Perkins, N.C., McLean, S.G., 2016. Quantifying performance and effects of load carriage during a challenging balancing task using an array of wireless inertial sensors. Gait Posture 43, 65–69.

Cancio, J.M., Oliver, R.A., Yancosek, K.E., 2017. Functional capacity evaluation-military: program description and case series. Mil. Med. 182 (1/2), e1658–e1664.

Freedland, R.L., Bertenthal, B.I., 1994. Developmental changes in interlimb coordination: transition to hands-and-knees crawling. Psychol. Sci. 5 (1), 26–32.

Hildebrand, M., 1989. The quadrupedal gaits of vertebrates. Bioscience 39, 766–775.

Jaworski, R.L., Jensen, A., Niederberger, B., Congalton, R., Kelly, K.R., 2015. Changes in combat task performance under increasing loads in active duty marines. Mil. Med. 180 (3), 179–186.

Kano, T., Owaki, C., Ishiguro, A., 2012. Reconsidering inter- and intra-limb coordination mechanisms in quadruped locomotion. Proceedings of the 2012 IEEE/RSJ International Conference on Intelligent Robots and Systems. Vilamoura, Algarve [Portugal].

Kaufman, L., Rousseeuw, P.J., 1990. Finding Groups in Data: An Introduction to Cluster Analysis. Wiley, New York.

Kumar, V., Chhabra, J.K., Kumar, D., 2014. Performance evaluation of distance metrics in the clustering algorithms. J. Comput. Sci. 13 (1), 38–52.

Larsen, B., Netto, K., Skovli, D., Vincs, K., Vu, S., Aisbett, B., 2012. Body armor, performance, and physiology during repeated high-intensity work tasks. Mil. Med. 177 (11), 1308–1315.

Larsen, B., Netto, K., Aisbett, B., 2014. Task-specific effects of modular body armor. Mil. Med. 179 (4), 428–434.

McElroy, E.J., Hickey, K.L., Reilly, S.M., 2008. The correlated evolution of biomechanics, gait and foraging mode in lizards. J. Exp. Biol. 211 (7), 1029–1040.

McGhee, R.B., 1968. Some finite state aspect of legged locomotion. Math. Biosci. 3, 331–351.

McGinnis, R.S., Cain, S.M., Davidson, S.P., Vitali, R.V., Perkins, N.C., McLean, S.G., 2016. Quantifying the effects of load carriage and fatigue under load on sacral kinematics during countermovement jump with IMU-based method. Sports Eng. 19, 21–34.

McGinnis, R.S., Cain, S.M., Davidson, S.P., Vitali, R.V., McLean, S.G., Perkins, N.C., 2017. Inertial sensor and cluster analysis for discriminating agility run technique and quantifying changes across load. Biomed. Signal Process. Control 32, 150–156.

Mitchell, K.B., Batty, J.M., Coyne, M.E., DeSimone, L.L., Bensel, C.K., 2016. Reliability Analysis of Time to Complete the Obstacle Course Portion of the Load Effects Assessment Program (LEAP). NATICK/TR-17/002. Natick Soldier Research, Development, and Engineering Center (NSRDEC), Natick, MA.

Ojeda, L., Zaferiou, A.M., Cain, S.M., Vitali, R.V., Davidson, S.P., Stirling, L.A., Perkins, N.C., 2017. Estimating stair running performance using inertial sensors. Sensors 17 (11).

O'Neal, E.K., Hornsby, J.H., Kelleran, K.J., 2014. High-intensity tasks with external load in military applications: a review. Mil. Med. 179 (9), 950–954.

Owaki, D., Kano, T., Nagasawa, K., Tero, A., Ishiguro, A., 2012. Simple robot suggests physical interlimb communication is essential for quadruped walking. J. R. Soc. Interf., 78

Owaki, D., Ishiguro, A., 2017. A quadruped robot exhibiting spontaneous gait transitions from walking to trotting to galloping. Sci. Rep. (Nature Publisher Group) 7, 1–10.

Patrick, S.K., Noah, J.A., Yang, J.F., 2009. Interlimb coordination in human crawling reveals similarities in development and neural control with quadrupeds. J. Neurophysiol. 101 (2), 603–613.

Patrick, S.K., Noah, J.A., Yang, J.F., 2012. Developmental constraints of quadrupedal coordination across crawling styles in human infants. J. Neurophysiol. 107 (11), 3050–3061.

Raibert, M.H., 1986. Legged Robots that Balance. The MIT Press, Cambridge, Massachusetts.

Righetti, L., Nylén, A., Rosander, K., Ijspeert, A.J., 2015. Kinematic and gait similarities between crawling human infants and other quadruped mammals. Front. Neurol. 6, 1–11. Article 17.

Rousseeuw, P.J., 1987. Silhouettes: a graphical aid to the interpretation and validation of cluster analysis. J. Comput. Appl. Math. 20, 53–65.

Schermann, H., Karakis, I., Dolkart, O., Maman, E., Kadar, A., Chechik, O., 2017. Olecranon bursitis in a military population: epidemiology and evidence for prolonged morbidity in combat recruits. Mil. Med. 182 (9/10), e1976–e1980.

Schwartz, O., Malka, I., Olsen, C.H., Dudkiewicz, I., Bader, T., 2018. Overuse Injuries in the IDF's combat training units: rates, types, and mechanisms of injury. Mil. Med. 183 (3/4), e196–e200.

Song, S., Walkdron, K., 1989. Machines that Walk: The Adaptive Suspension Vehicle. The MIT Press, Cambridge, Massachusetts.

Tack, D., Kelly, A., Richter, M., Bray-Miner, J., 2012. Preliminary results of MC-LEAP testing of U.S. Marine Combat Load Order Configurations. ONR Contract Report No. N00014011-C-0206.

Tammana, A., McKay, C., Cain, S.M., Davidson, S.P., Vitali, R.V., Ojeda, L., Stirling, L., Perkins, N.C., 2018. Load-embedded inertial measurement unit reveals lifting performance. J. Appl. Ergon. 70, 68–76.

Wannier, T., Bastiaanse, C., Colombo, G., Dietz, V., 2001. Arm to leg coordination in humans during walking, creeping and swimming activities. Exp. Brain Res. 141 (3), 375–379.

Wold, S., Esbensen, K., Geladi, P., 1987. Principal component analysis. Chemom. Intell. Lab. Syst. 2 (1), 37–52.

Zaferiou, A.M., Ojeda, L., Cain, S.M., Vitali, R.V., Davidson, S.P., Stirling, L.A., Perkins, N.C., 2017. Quantifying performance on an outdoor agility drill using foot-mounted inertial measurement units. PLoS ONE 12 (11).